Correlation Analysis of COMAMMOX *Nitrospira* Relative to AOB Activity in Biological Nitrogen Removal from Synthetic Municipal Wastewater Using Full Factorial Design

Tristan Roy L. Panaligan[1,2,3,*], Yi-Ju Wu[4], Bonifacio T. Doma, Jr.[1,2], and Liang-Ming Whang[5,6]

[1]School of Chemical, Biological, Materials Engineering and Sciences, Mapúa University, Manila, 1002, Philippines
[2]School of Graduate Studies, Mapúa University, Manila, 1002, Philippines
[3]Mapúa Institute of Technology at Laguna, Mapúa Malayan Colleges Laguna, Laguna, 4025, Philippines
[4]Department of Safety, Health and Environmental Engineering, National United University, 2, Lienda, Miaoli 36063, Taiwan, China
[5]Department of Environmental Engineering, National Cheng Kung University, Tainan City, 70101, Taiwan, China
[6]Sustainable Environment Research Laboratory, National Cheng Kung University, Tainan 70101, Taiwan, China
Email: trlpanaligan@mymail.mapua.edu.ph (T.R.L.P.); ccdjessica@nuu.edu.tw (Y.-J.W.); btdoma@mapua.edu.ph (B.T.D.); whang@mail.ncku.edu.tw (L.M.W.)
*Corresponding author

Manuscript received February 26, 2025; revised March 13, 2025; accepted April 19, 2025; published July 7, 2025

***Abstract*—This study explores the role of Comammox *Nitrospira* (CMX) in ammonia-nitrogen removal from synthetic municipal wastewater, with a focus on key operational parameters: initial ammonia concentration (N_o), COD/N ratio, and pH. A Full Factorial Design (FFD) of Experiments was implemented to systematically evaluate the effects of these factors on nitrification efficiency. Microbial population dynamics were assessed using DNA and rRNA qPCR analyses, providing insights into the relative abundance and activity of CMX in comparison to Ammonia Oxidizing Bacteria (AOB). The experimental results suggest that CMX plays a dominant role in ammonia oxidation, as indicated by minimal nitrite accumulation across all conditions. The optimal experimental condition (N_o = 60 mg/L, COD/N = 0.5, pH = 8.6) was identified through a prediction profiler function. Statistical modeling confirmed that ammonia removal was significantly influenced by the tested parameters (*p* = 0.0124, F-ratio = 3797.377), whereas nitrate formation exhibited less variation and was not statistically significant (*p* = 0.4121, F-ratio = 3.0531). These findings contribute to a deeper understanding of complete ammonia oxidation and its implications for optimizing biological nitrogen removal in wastewater treatment systems.**

***Keywords*—Comammox *Nitrospira*, nitrification, biological nitrogen removal, ammonia oxidation, Full Factorial Design, microbial population dynamics, qPCR analysis**

I. Introduction

The evident redox sensitivity of nitrogen leads to its transformation into several significant compounds, which include ammonia (NH_3), ammonium (NH_4^+), nitrate (NO_3^-), and nitrite (NO_2^-) apart from nitrogen gas (N_2) [1]. Ammonium ions represent the primary nitrogen pollution form extensively found in water systems [2]. High concentrations of ammonia or ammonium-nitrogen (NH_4-N) in water can be toxic to aquatic organisms, particularly fish and invertebrates [3]. It interferes with their respiratory systems, impairs growth, and can lead to mortality, disrupting the natural balance of aquatic ecosystems. Studies have shown that elevated concentrations of ammonium ions cause harm to aquatic life, illustrating the toxicity of ammonia even at very low levels, such as 0.2 mg/L, to as high as 17.1 mg/L, just as in Chinese surface waters [4]. Therefore, the significant concern lies in the toxicity of ammonia in aquatic environments [5], especially in areas densely populated by humans or housing large populations of farm animals.

NH_4-N, along with other nutrients, contributes to eutrophication when present in excess. This excess nutrient load stimulates the overgrowth of algae and other aquatic plants, leading to algal blooms [6]. Algal blooms alter the balance of aquatic ecosystems, causing changes in species composition, reducing sunlight penetration, and depleting oxygen levels as the algae decompose. This decrease in dissolved oxygen can harm fish and other aquatic organisms, leading to fish kills and the loss of biodiversity [7]. Maharjan *et al.* [8] reported that elevated levels of NH_4^+-N in drinking water sources can pose health risks to humans. Although ammonia may not be directly harmful at typical environmental levels, it can react with other chemicals during water treatment, forming disinfection byproducts that pose health risks. Elevated nitrate levels in drinking water can lead to methemoglobinemia (blue baby syndrome), reducing an infant's oxygen-carrying capacity [9].

Municipal Wastewater (MWW) refers to the used water and waste generated from households, businesses, and institutions in a city or even urban area [10], which is collected, treated, and disposed of through public sewage systems and treatment facilities. MWW undergoes treatment in Sewage Treatment Plants (STPs) or Wastewater Treatment Plants (WWTPs) to remove contaminants and make them safe for release back into the environment. Ongoing research and technological advancements focus on improving wastewater treatment efficiency, reducing energy consumption, minimizing environmental impacts, and developing innovative solutions for wastewater treatment and resource recovery.

Mathew *et al.* [11] highlighted that Biological Nitrogen Removal (BNR) processes are essential in wastewater treatment to reduce nitrogen compounds, primarily ammonia and nitrate. BNR aligns with sustainable wastewater treatment practices due to its reduced reliance on chemical agents. It offers a more environmentally friendly approach, contributing to the overall sustainability of WWTPs. BNR methods are gaining attention due to their cost-effectiveness compared to chemical-intensive approaches. This economic advantage makes them attractive for both existing and new wastewater treatment facilities [12].

BNR methods are versatile and applicable in various

doi: 10.18178/ijesd.2025.16.4.1531

wastewater treatment settings, including municipal wastewater treatment plants and industrial facilities. Fontalvo *et al.* [13] described the long-standing model of nitrification as a two-step process mediated by distinct microbial groups, including Ammonia-Oxidizing Bacteria (AOB) and Archaea (AOA), along with Nitrite-Oxidizing Bacteria (NOB). More recently, Daims *et al.* [14] identified members of the genus *Nitrospira* capable of COMplete AMmonia OXidation (COMAMMOX or CMX). Recently identified members of the *Nitrospira* genus participating in the complete ammonia oxidation process have been acknowledged, but their significance in engineered water treatment systems remains inadequately comprehended [15]. Despite this breakthrough, the effects of key operational parameters—such as initial ammonia concentration (N_0), Chemical Oxygen Demand to Nitrogen (COD/N) ratio, and pH—on CMX activity and its interactions with AOB remain underexplored. This knowledge gap limits the optimization of BNR processes and the potential integration of CMX into wastewater treatment strategies.

This study systematically investigates the influence of N_0, COD/N, and pH on CMX activity in synthetic municipal wastewater. Using quantitative polymerase chain reaction (qPCR) for DNA- and RNA-based assessments, the study quantifies microbial abundance and metabolic activity to clarify CMX-AOB interactions. A Full Factorial Design (FFD) is applied to assess both individual and interactive effects of these parameters on ammonia removal and nitrate formation, while statistical modeling (JMP® by SAS Institute) identifies optimal conditions for enhanced nitrogen removal. This research provides one of the first structured evaluations of CMX-driven nitrification under controlled conditions, integrates molecular quantification techniques to link microbial abundance with function, and utilizes FFD to improve understanding of CMX-AOB interactions. Additionally, this research aligns with the United Nations Sustainable Development Goals (SDGs), particularly Goal 6 (Clean Water and Sanitation) by improving water quality and Goal 14 (Life Below Water) by minimizing nutrient pollution in aquatic ecosystems.

II. Literature Review

A. Nitrification Process of Biological Nitrogen Removal

Nitrification is highly sensitive to environmental factors such as pH, temperature, oxygen levels, and organic matter. For instance, nitrification rates are optimal in neutral to slightly alkaline conditions and moderate temperatures, while extreme pH levels and low temperatures can inhibit the activity of nitrifying microorganisms [16, 17]. Oxygen is a crucial factor as both AOB and NOB require aerobic conditions to thrive [18].

Ward [19] discussed that in aerobic conditions, autotrophic AOB, AOA, and NOB collectively facilitate the conversion process. Zheng *et al.* [20] noted that microbial communities typically thrive in diverse and intricate ecosystems, where species interact and their genomic capabilities evolve. While the comprehension of species interaction and evolution has advanced in recent decades, most studies on evolutionary dynamics primarily focus on individual species in isolation or within experimental systems comprising only a limited number of interacting species. All identified CMX organisms fall within the *Nitrospira* genus, exhibiting a comprehensive genetic complement encompassing both ammonia and nitrite oxidation processes [21].

B. Nitrification Factors and Microbial Dynamics

Nitrification is influenced by several critical factors, including temperature, pH, oxygen concentration, and substrate availability [22]. pH also affects nitrification rates, with most nitrifiers thriving in a pH range of 7.0 to 8.5, outside of which their activity diminishes significantly [23]. Prosser and Nicol [24] reported that ammonium oxidation is entirely halted at pH 5, whereas nitrite oxidation is significantly hindered at pH 8.5. Unlike AOB, NOB is seldom inhibited at low pH levels. Oxygen concentration is another crucial factor, as nitrification is an aerobic process; thus, sufficient dissolved oxygen levels are essential for the survival and activity of nitrifying microorganisms [25]. Furthermore, substrate availability, including the concentrations of ammonia and nitrite, directly impacts the nitrification process, as these substrates are the primary sources of energy for autotrophic microorganisms [26].

Zielinska *et al.* [27] scrutinized the impact of COD/N and DO on nitrification and denitrification efficiency. The findings revealed an intricate relationship, indicating that higher COD/N values exhibit an inverse correlation with nitrification efficiency and a direct correlation with denitrification efficiency. Specifically, they studied the impact of the carbon-to-nitrogen ratio and DO concentration on nitrogen removal efficiency using two parallel Sequencing Batch Reactors (SBRs). The study demonstrated that ammonia oxidation efficiency consistently exceeded 90%, yielding nitrates as the primary product, regardless of DO levels (0.5 and 1.5 mg O_2/L). However, the highest nitrogen removal efficiency, surpassing 0%, was observed at a COD/N ratio of 6.8 with a DO concentration of 0.5 mg O_2/L.

C. Design of Experiments

Román-Ramírez *et al.* [28] emphasized that a robust experimental design is critical for the development of any product or process, necessitating a deep comprehension of the system under investigation. Design of Experiments (DOE) is a statistical methodology with a primary focus on its development by Sir Ronald Fischer for agricultural purposes in the 1920s [29]. This statistical methodology involves a suite of applied tools to systematically unveil cause-and-effect relationships within studied processes. Extending beyond its agricultural origins, DOE has become a fundamental tool widely employed across various scientific and industrial domains, particularly in product and process design, development, and optimization [30].

One prominent DOE methodology, the FFD, merits special attention. This approach systematically examines all possible combinations of factor levels, providing a comprehensive understanding of the interactions between variables [31]. For investigating k independent factors at two levels each, the total number of experiments is 2^k [32]. The 2^k FFD is especially advantageous in preliminary experimental phases, particularly when the count of process or design parameters (factors) is four or less [33] and is commonly used for screening studies [34].

III. Materials and Methods

A. Sludge Samples

The study used wastewater sludge obtained from the municipal wastewater treatment plant in Yongkang District, Tainan, Taiwan, between May 2023 and July 2023. This source was chosen due to its representative characteristics and relevance to one of the study's objectives: determining the proper ratio of CMX *Nitrospira* and AOB in the wastewater. Sludge samples were collected from the secondary treatment process of the selected municipal wastewater treatment plant.

This testing process was carried out by personnel affiliated with the National Cheng Kung University (NCKU) – Department of Environmental Engineering, specifically the Environmental Biotechnology Laboratory (EBL). After quantifying both bacterial populations, it will aid in the idea that their ratio influences the removal rate of ammonia-nitrogen can be conducted. At this point, the sludge is identified as the "Analyzed Sludge" (AS).

B. Synthetic Municipal Wastewater

The Synthetic Municipal Wastewater (SMW) was prepared according to the concentrations specified by NCKU-EBL, as presented in Table 1. This ensured that the experimental conditions closely simulated real-world scenarios, leading to meaningful and applicable research outcomes.

Table 1. Contaminant concentrations in simulated municipal wastewater

Chemical / Contaminant	Final Synthetic Wastewater Concentration [FSWC] (mg / L)
KH_2PO_4	0.1760
Na_2CO_3	1.7500
$MgSO_4.7H_2O$	0.0508
$CaCl_2.4H_2O$	0.0037
$MnCl_2.4H_2O$	0.0028
$ZnSO_4.7H_2O$	0.0044
$CuSO_4.5H_2O$	0.0039
$FeCl_3.6H_2O$	0.0242
$NaMo_4.2H_2O$	0.0010

Careful measurement and mixing techniques were employed to achieve the desired concentrations, minimizing potential variability and ensuring consistency across experimental replicates. The synthetic wastewater was prepared by combining calculated volumes, labeled as Stock Solution Volume (SSV), of various component stock solutions in a 500 mL volumetric flask and filling it to the mark, creating an intermediate wastewater concentration. The contents are then transferred to a suitable container for storage.

C. Nitrogen and Carbon Source

A nitrogen stock solution was prepared by dissolving 0.3000 grams of ammonium chloride (NH_4Cl) in 50 mL of deionized water to create a 6000 mg/L NH_4^+-N solution. For the carbon source, a glucose ($C_6H_{12}O_6$) stock solution was made by dissolving 0.3500 grams of glucose in 50 mL of deionized water, resulting in a concentration of 7000 mg/L.

D. Batch Bioreactor Experiments

When the SMW is required for use, an additional dilution is performed by extracting 100 mL from the intermediate concentration, transferring it into a 2-L volumetric flask, and diluting it to the mark. This step yields the final concentration of the synthetic wastewater, which is then ready for utilization in batch experiments specific to the nitrification process. The final dilution step should be carried out as often as needed to guarantee the consistency and reliability of the synthetic wastewater for experimental use. Each bioreactor setup comprises a 1-liter Pyrex glass container constructed to mimic the design depicted in Fig. 1.

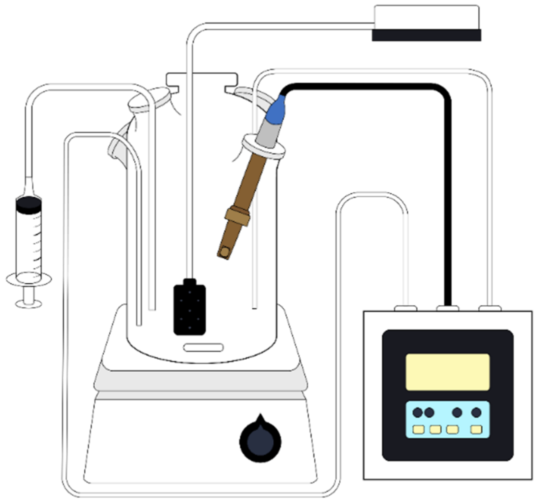

Fig. 1. Schematic drawing of a bioreactor setup.

A 500-mL AS sample is measured in an Imhoff sedimentation cone and split into two 250-mL centrifuge bottles for easier handling. Settling is accelerated using a Sorvall LYNX 4000 Superspeed Centrifuge (ThermoFisher Scientific) at 10,000 rpm for 5 min. The centrifuged contents are returned to the Imhoff cone, the supernatant is removed, and the sludge is resuspended to 500 mL with DI water. The prepared sample is then transferred to a 1-L Pyrex glass container that serves as the bioreactor to initiate the experimental run. 50 mL of synthetic wastewater is first added to the bioreactor, followed by activating the stirring equipment at Level 5 to ensure uniform mixing. The aeration source is then placed into the reactor and turned on, followed by the addition of 350 mL of deionized (DI) water.

A pH probe is strategically positioned for continuous monitoring of the bioreactor's internal pH. The pH Control System is switched on, and the probe, along with tubing for the NaOH solution, is inserted to facilitate auto-pH adjustment based on the preassigned pH setpoint. To introduce essential substrates, 50 mL of glucose solution and 50 mL of NH_4Cl solution (both prepared from their respective intermediate concentrations per leg) are added to the reactor. Once all preparations are complete, sampling is conducted at all declared time points, using a 20-mL syringe for consistent collection of bioreactor contents at regular intervals. The collected samples are transferred to designated containers for post-batch analysis, with syringe usage frequency per sampling point determined based on Table 2.

The collected samples were filtered through a 0.45 μm syringe filter into 25-mL centrifuge tubes and stored at 4°C to preserve stability for analysis. The bioreactors were then configured with varying N_0, COD/N, and pH levels according to the experimental FFD (Table 3) to represent different parameter combinations.

Table 2. Sample container specifics

Container	Sampling Time Points	Sampling Purpose from Batch Experiments
50 mL centrifuge tube	ALL	UV-Vis spectrophotometry to analyze NH_4-N, NO_2-N, NO_3-N,
50 mL centrifuge tube	0 h	MLSS/MLVSS testing
2 mL Eppendorf tube	ALL	DNA / RNA analyses

This setup ensures controlled manipulation of specified parameters, allowing for systematic experimentation and analysis. The established parameter combinations, referred to as "legs", provide clarity and consistency throughout the study, facilitating further evaluation of the bioreactor system.

Two levels for each factor were determined according to several literatures. The negative level (-) represents the lower value of the factors, and the positive level (+) represents the higher value. The N_0 covers a range of 30 to 60 g/mL; the initial COD/N ratio is between 0.5 to 4.5, and the pH is from 7 to 8.6.

Table 3. DOE matrix of the study

Leg	Pattern			N_0 (mg/L)	Initial COD/N	pH
1	-	-	-	30	0.5	7.0
2	-	-	+	30	0.5	8.6
3	-	+	-	30	4.5	7.0
4	+	-	-	30	4.5	8.6
5	+	+	-	60	0.5	7.0
6	+	-	+	60	0.5	8.6
7	-	+	+	60	4.5	7.0
8	+	+	+	60	4.5	8.6

E. Post-Batch Experiment Sample Analyses and Testing

Upon the conclusion of the batch experiments, the concentrations of nitrogen species in the collected samples were determined using UV-Vis Spectrophotometry. Specifically, NH_4-N will be quantified by the Indophenol Method, utilizing UV-Vis to detect the formation of the indophenol blue complex, providing sensitive and accurate measurements. The Griess Method was employed for NO_2-N analysis, in which nitrite reacts to form a colored azo dye, detectable at a specific wavelength using a spectrophotometer. Finally, NO_3-N was measured using the 4500-NO_3^- B Method, which uses direct UV absorbance to quantify nitrate without interference from other nitrogen species.

In addition to nitrogen species testing, DNA and RNA analyses were performed at multiple time points to quantify microbial populations, including AOB and CMX Nitrospira, allowing for the tracking of bacterial growth and activity. Sludge samples were collected from batch tests (referencing again from Table 2), centrifuged, and stored at -20°C and -80°C, respectively, before extraction. DNA and RNA were extracted using the DNeasy PowerSoil Kit (Qiagen, Valencia, CA, USA) and the RNeasy Mini Kit (Qiagen), ensuring accurate molecular characterization of microbial dynamics.

After extraction, DNA was purified using the QIAquick PCR Purification Kit, while RNA was treated with the RNase-Free DNase Set (Qiagen) and subsequently used in the reverse transcription reaction with the PrimeScript™ RT Reagent Kit (TaKaRa, Japan) along with Random 6-mers and Oligo dT Primer, following the manufacturer's instructions. The PCR program was set to 37°C for 15 min, followed by 85°C for 5 s. Both DNA and complementary DNA (cDNA) were stored at -20°C prior to further analysis.

The qPCR analyses targeting the amoA gene of AOB and CMX in both DNA and cDNA were performed in triplicate using amoA 1F/amoA 2R [35] for AOB and amoA AF/amoA SR [36] for Comammox. The qPCR standards were prepared using plasmids extracted from clones containing partial amoA gene sequences of AOB and Comammox, which were amplified from environmental samples and confirmed through sequencing and BLAST analysis against the NCBI database.

The LightCycler 480 II (Roche) was used for qPCR analysis with LightCycler 480 SYBR Green I Master (Roche). The thermal conditions for AOB amoA gene quantification were as follows: 95°C for 10 min, followed by 50 cycles of 95°C for 10 s, 55°C for 20 s, and 72°C for 20 s (detection), followed by a melting curve analysis from 65°C to 95°C with a heating rate of 0.11°C/s. The thermal conditions for CMX amoA gene quantification were as follows: 95°C for 10 min, followed by 60 cycles of 95°C for 10 s, 58°C for 20 s, and 72°C for 20 s (detection), followed by melting curve analysis from 65°C to 95°C with a heating rate of 0.11°C/s. The RNA CMX/AOB ratio was calculated by dividing the transcribed cDNA copy numbers of CMX and AOB.

Standard methods to perform Mixed Liquor Suspended Solids (MLSS) and Mixed Liquor Volatile Suspended Solids (MLVSS) testing were also performed using samples collected at time zero (0 hr) to establish initial biomass concentrations in the reactors, which are crucial for assessing the overall performance of the BNR process.

F. Statistical Analysis of Data

This study employs statistical methods to evaluate the effects of initial NH_3-N concentration, COD/N ratio, and pH on the RNA CMX/AOB ratio.

Analysis of Variance (ANOVA) was applied to analyze the statistical significance of these effects, while regression modeling provided a quantitative understanding of the relationships between the factors and the RNA CMX/AOB ratio. The Actual vs. Predicted plot in JMP is widely used to evaluate model performance by comparing predicted values to observed data points. Sjah *et al.* [37] and Liemohn *et al.* [38] pointed out the importance of assessing model accuracy, particularly through metrics such as the coefficient of determination (R^2) [39] and the Root Mean Square Error (RMSE) [40]. The R^2 assesses the goodness of fit in a regression model by quantifying how well predicted values approximate actual data. It indicates the proportion of variance explained by independent variables, making it essential for evaluating predictive accuracy. The RMSE measures the dispersion of residuals, with lower values indicating better model precision. The results also aim to clarify the critical operational factors affecting Comammox *Nitrospira* activity in synthetic wastewater treatment systems.

IV. Result and Discussion

A. Volatile Suspended Solids Concentration

Fig. 2 depicts the starting data of Volatile Suspended Solids (VSS) for each of the parameter combinations. The initial VSS values ranged from 2,440 mg/L to 3,876 mg/L and showed significant variation based on the combined effects of N_0, COD/N ratio, and pH.

During the start-up phase, the biomass originated from microorganisms naturally present in the feed wastewater, as the reactor was not seeded with external inoculum. At an N_0 of 30 mg/L and a COD/N ratio of 0.5, VSS levels were relatively low, ranging between 2,440 mg/L and 2,536 mg/L, except for Leg 4. Increasing the COD/N ratio to 4.5 resulted in a significant rise in VSS levels, peaking at 3,876 mg/L at a pH of 8.6, suggesting that higher carbon availability and an alkaline pH create more favorable conditions for biomass growth. At a higher N_0 of 60 mg/L, VSS concentrations increased further as compared with Leg 1 to 3, likely due to the adaptation to greater nutrient availability and the stimulation of microbial activity by the elevated substrate levels.

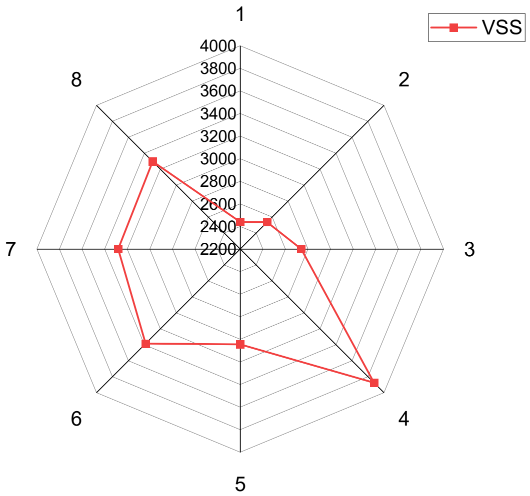

Fig. 2. VSS concentration per leg at time zero.

For a COD/N ratio of 0.5, VSS concentrations ranged from 3,044 mg/L to 3,384 mg/L, while a COD/N ratio of 4.5 yielded slightly higher values, between 3,280 mg/L and 3,296 mg/L. The highest initial VSS value occurred under conditions of Leg 4. This suggests that the interaction of factors may have created the most favorable initial conditions for microbial abundance.

B. DNA CMX Relative Abundance to AOB at Time Zero

Fig. 3 presents the DNA qPCR analysis of CMX and AOB populations at time zero, displayed on a logarithmic scale. The CMX/AOB ratio, calculated from the original CMX and AOB copy numbers (in copy/mL) to reflect their relative abundance, ranged from 29.05 to 166.27 throughout the experiment. This combined approach enhances interpretability and aligns with standard practices in qPCR data presentation, allowing for a more meaningful comparison of population dynamics across different experimental conditions.

At a lower initial ammonia-nitrogen concentration of 30 mg/L, the CMX/AOB ratios remained below 50, with the lowest value observed at Leg 1. This suggests that at low nutrient levels, AOB maintains a relatively higher population, likely due to reduced nitrogen availability limiting CMX dominance. As pH or COD/N increased, as in Leg 3, the ratio rose to 49.86, indicating enhanced conditions for CMX activity, potentially due to the increased availability of organic carbon.

In contrast, higher initial ammonia-nitrogen concentrations of 60 mg/L led to significantly higher CMX/AOB ratios, peaking at 166.27 in Leg 6. This suggests that elevated nutrient levels strongly favor CMX populations, particularly when organic carbon is limited. A similar trend is observed in Leg 5, with a relative amount of CMX to AOB value of 165.32. However, at higher COD/N ratios, the DNA CMX/AOB ratios slightly declined, as seen in Leg 7 and Leg 8. The marked drop in Leg 8, despite high nutrient levels, highlights the influence of pH and COD/N interactions, where an elevated pH of 8.6 may have created conditions more favorable to AOB, reducing the dominance of CMX.

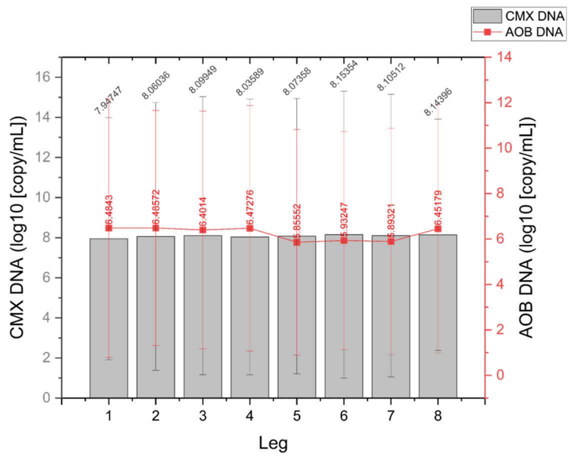

Fig. 3. Quantification of CMX and AOB DNA by qPCR.

C. RNA CMX Relative Abundance to AOB vs NH_4-N, NO_3-N, and NO_2-N Trends over Time

Fig. 4 illustrates the temporal trends of NH_4-N, NO_2-N, and NO_3-N concentrations, along with the RNA CMX/AOB ratio. NH_4-N concentrations exhibited a distinct and consistent decline across all, as shown in Fig. 4a, confirming active nitrification. The rate of ammonia removal was notably higher in Legs 1–4, which had an initial NH_4^+-N concentration of 30 mg/L, with concentrations at 60 min (T60) ranging from 6.86 mg/L to 19.24 mg/L. Among these, Leg 3 exhibited the highest Specific Nitrogen Removal Rate (SNRR) of 8.72 mgN/L/hr/gVSS. Conversely, legs with lower COD/N ratios, such as Leg 1, showed slower removal rates, likely due to the influence of lower pH and limited organic carbon availability, resulting in a lower SNRR of 5.16 mgN/L/hr/gVSS.

For the legs with an initial NH_4^+-N concentration of 60 mg/L, ammonia removal was comparatively slower, with concentrations ranging from 39.11 mg/L Y to 45.43 mg/L. Leg 8 showed a specific nitrogen removal rate of 6.69 mgN/L/hr/gVSS, which was the highest among Legs 5 and 8 alone. The lower COD/N ratio and neutral pH conditions in Legs 5 and 7 resulted in slower ammonia removal, with specific nitrogen removal rates of 4.12 and 4.87 mgN/L/hr/gVSS, respectively.

As shown in Fig. 4b, nitrite accumulation remained minimal across most experimental legs throughout the study, suggesting a direct transformation of ammonia into nitrate, potentially bypassing the conventional two-step nitrification pathway. The low nitrite levels observed in this study suggest that CMX may contribute to a more direct and efficient ammonia-to-nitrate conversion. This trend was particularly evident in Legs 1–4, where nitrite levels were consistently low, indicating that ammonia oxidation was tightly coupled with nitrate formation. Traditionally, nitrification has been understood as a sequential process involving AOB converting ammonia to nitrite, followed by NOB transforming nitrite into nitrate. However, this concept has been revised with the discovery of a unique subgroup within the *Nitrospira* genus, specifically within sub-lineage II, which can perform complete ammonia oxidation within a single cell [21]. The near absence of nitrite suggests that CMX played a dominant role in facilitating a rapid, single-step conversion of ammonia to nitrate, minimizing the intermediate accumulation typically observed in AOB-NOB systems. Even in Legs 5–8, nitrite remained largely undetectable or fluctuated slightly. The only notable exceptions were Leg 2, where nitrite accumulated to 0.3357 mg/L at T60, and Leg 6, where it peaked at 0.8163 mg/L at 30 min (T30) before rapidly declining. These brief accumulations indicate a temporary lag in nitrite oxidation relative to ammonia oxidation, which is somewhat balanced by nitrate formation.

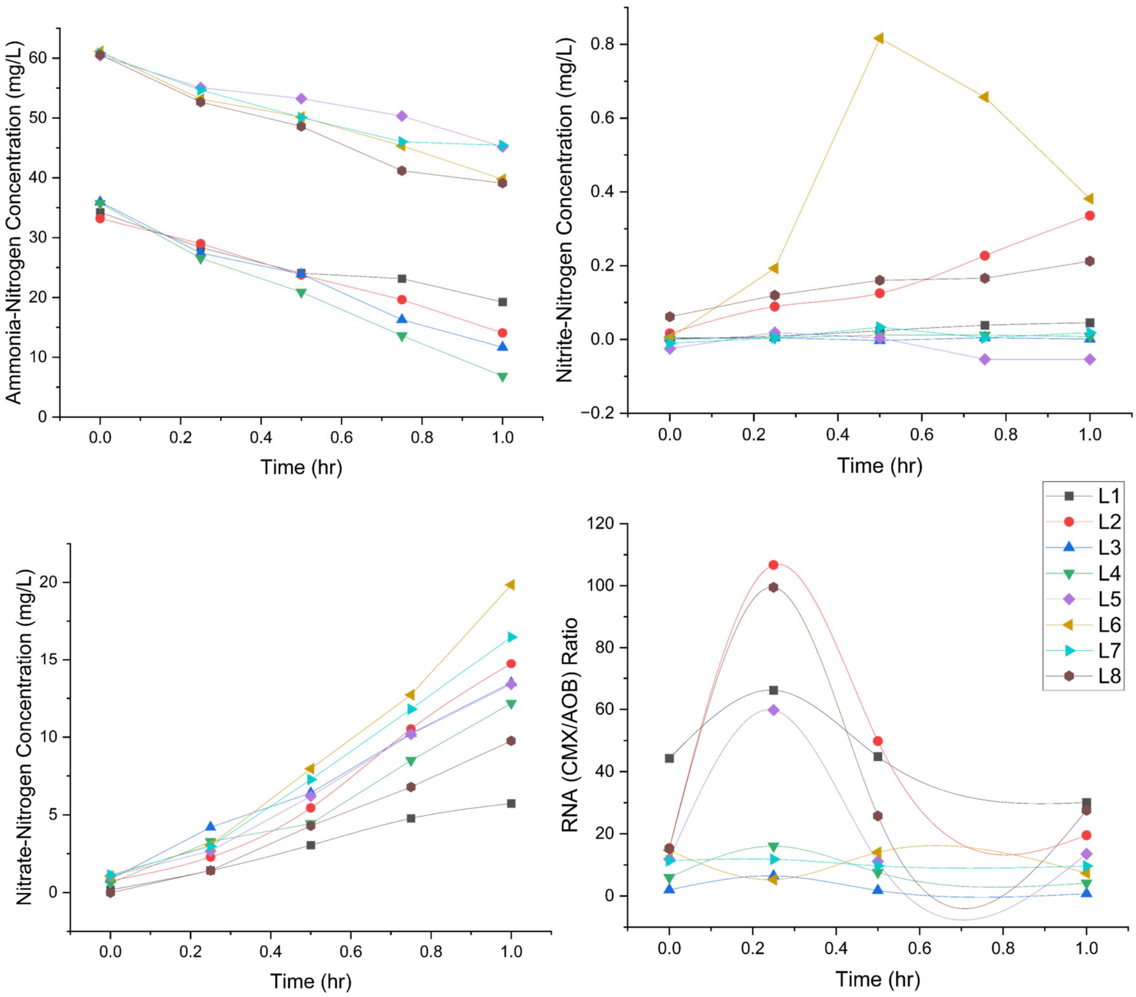

Fig. 4. Temporal trends in (a) NH_4-N, (b) NO_2-N, (c) NO_3-N concentrations, and (d) RNA ratio (CMX/AOB).

As nitrification progressed, NO_3-N concentrations gradually increased over time in all legs, as depicted in Fig. 4c. The nitrate concentrations at T60 of Legs 2–4 varied between 12.18 mg/L and 14.74 mg/L, whereas Leg 1 is quite low at 5.73 mg/L. Despite the nitrite buildup in Leg 2, the overall nitrate accumulation suggests that nitrification remained balanced. Higher COD/N ratios and elevated pH levels positively influenced nitrification efficiency, as evidenced by Leg 4, which demonstrated improved ammonia removal and nitrate formation. The nitrate levels for Legs 5–8 were significantly higher, reaching 19.85 mg/L in Leg 6 and 16.47 mg/L in Leg 7. The highest nitrate accumulation in Leg 6 aligns with its high nitrite buildup, indicating active AOB activity with slightly delayed nitrite oxidation. Leg 8 showed less nitrate accumulation than anticipated, even though its initial ammonia concentration, COD/N ratio, and pH were all quite high. This deviation implies that increased substrate availability may have changed microbial activity, even though high COD/N and alkaline circumstances typically encourage nitrification. Possible causes include microbial competition, in which heterotrophs outcompete nitrifiers for oxygen and nutrients, and ammonia inhibition, in which elevated ammonia levels momentarily limit AOB function.

As for the RNA activity result trends, it can be viewed in Fig. 4d. In Leg 1, the RNA CMX/AOB ratio peaked at T15 before gradually declining by T60, suggesting that CMX activity was initially supported under these conditions but may have diminished due to substrate depletion or metabolic shifts. Leg 2, which had the same COD/N ratio but a higher pH of 8.6, exhibited a sharper RNA peak at T15 (106.69) before significantly dropping to 19.53 at T60. The temporary boost in CMX activity under alkaline conditions suggests that high pH initially enhanced ammonia oxidation potential, but prolonged exposure may have imposed inhibitory effects.

In Legs 3 and 4, where the COD/N ratio was increased to 4.5, RNA activity was significantly lower. In Leg 3, the RNA ratio at T15 (6.48) was much lower than in Legs 1 and 2, decreasing further to 0.76 at T60, suggesting that the increased COD/N ratio may have restricted oxygen availability, potentially limiting CMX activity. Leg 4, at pH 8.6, exhibited a slightly higher RNA peak at T15 compared to Leg 3 but a similar decline to 4.16 at T60, further supporting the hypothesis that high COD/N conditions may suppress CMX activity due to competitive interactions and increased metabolic demands. In Legs 5 to 8, varied responses were observed. Leg 5 demonstrated moderate CMX activity, peaking at T15 (59.78) before decreasing to 13.54 at T60, indicating that while high nitrogen concentrations supported early metabolic activity, COD/N ratio and pH balance remained key for sustained CMX performance. Leg 6, with an increased pH of 8.6, showed irregular RNA trends, peaking at T30 before significantly dropping by T60. This suggests that an alkaline environment initially enhanced CMX activity but may not have been favorable for prolonged metabolic function when combined with a low COD/N ratio.

For the legs with a high COD/N ratio of 4.5, Leg 7 reached its peak RNA activity at T15 before gradually declining by T60, while Leg 8, despite its extreme initial parametric conditions, exhibited a sharp RNA peak at T15 (99.48) before significantly dropping to 27.55 at T60. This pattern suggests an initial microbial adaptation or stimulation, followed by a rapid decline, likely due to competitive microbial interactions, possible oxygen limitations (since DO was not in the monitoring parameters), or metabolic stress aggravated by the high COD/N conditions.

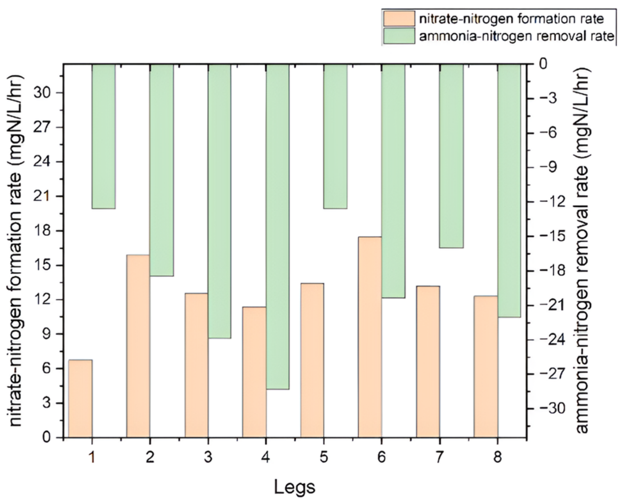

Fig. 5. NO_3-N formation rate vs NH_4-N removal rate.

Fig. 5 illustrates the comparative trends between nitrate-nitrogen formation and ammonia-nitrogen removal rates across different experimental legs. Notably, Legs 1 and 5 exhibit a marked discrepancy between these rates, likely attributable to their lower COD/N ratios and pH.

This suggests a potential limitation in microbial activity or efficiency in complete nitrification under these conditions. Similarly, Leg 7, despite having a higher initial ammonia concentration at 60 mg/L and a COD/N ratio of 4.5, shows a comparable trend, indicating that pH may be a more critical factor in influencing nitrification efficiency. The observed trends further reinforce the premise of a direct transformation of ammonia to nitrate, effectively bypassing significant nitrite accumulation. This aligns with findings on CMX organisms, which are capable of oxidizing ammonia to nitrate in a single-step process [21, 41, 42].

D. *Prediction Profiler Results and Statistical Analysis*

Fig. 6 presents the JMP prediction profiler, which serves as a tool for analyzing and visualizing the relationships between independent variables and the dependent variable in predictive models, such as regression or designed experiments [43]. This visualization aids in understanding the impact of each factor and its interactions with the response variable, providing valuable insights for optimizing the experimental conditions. Fig. 7 summarizes the least square fit results for the nitrate-nitrogen formation rate and ammonia-nitrogen removal rate comprised of the actual vs. predicted chart, summary of fit, ANOVA results, and effect tests. Based on the experimental results, Leg 6 exhibited the highest nitrate formation rate with a value of 17.45 mgN/L/hr and one of the highest ammonia removal rates at 20.34 mgN/L/hr, indicating efficient nitrification. Additionally, the ANOVA results suggest that ammonia removal was significantly influenced by the tested factors, reinforcing the reliability of the findings. Given that the JMP prediction profiler identified Leg 6 as the optimal setting, this aligns with the observed trends in the dataset. The high nitrate formation rate in Leg 6 supports the notion that complete ammonia oxidation occurred efficiently under its specific parameter combination.

E. *Discussion Highlights*

This study reinforces the emerging role of Comammox *Nitrospira* in biological nitrogen removal, particularly in the direct transformation of ammonia to nitrate, bypassing the conventional AOB-NOB two-step nitrification pathway. Daims *et al.* [13] and Kits *et al.* [40] similarly reported minimal nitrite accumulation in systems where *Nitrospira* species were capable of complete ammonia oxidation within a single organism [13, 44]. The findings of this study contradict the results of [45], which suggested that CMX *Nitrospira* gains a competitive advantage under low ammonium concentrations. Instead, higher initial NH_4-N levels resulted in increased DNA CMX/AOB ratios and enhanced ammonia removal rates, as observed in Leg 6. Conversely, lower ammonium concentrations corresponded to reduced DNA CMX/AOB ratios, with Leg 1 exhibiting the lowest ratio and a slower ammonia removal rate. Furthermore, the minimal nitrite accumulation across all experimental legs suggests that CMX facilitated a near-direct conversion of ammonia to nitrate, reinforcing its role in efficient nitrification.

The study's results indicate that nitrate formation rates were highest under conditions favoring CMX dominance, particularly in Leg 6, which achieved the highest nitrate formation rate of 17.45 mgN/L/hr. This is in contrast with [46], who reported that acidic pH enhances CMX metabolic activity. Additionally, [47] found that low COD/N ratios promote CMX activity over AOB, which corresponds to the high DNA CMX/AOB ratio (166.27) in Leg 6.

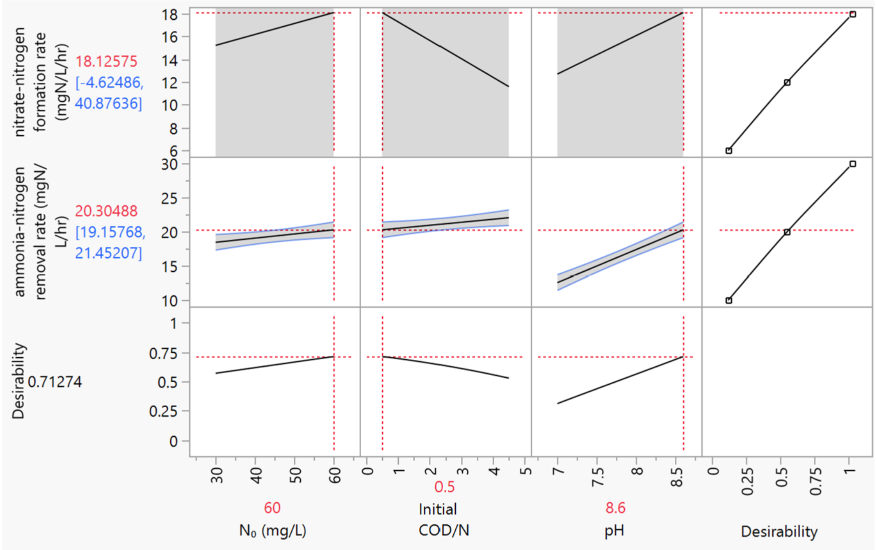

Fig. 6. Prediction profiler results of the study.

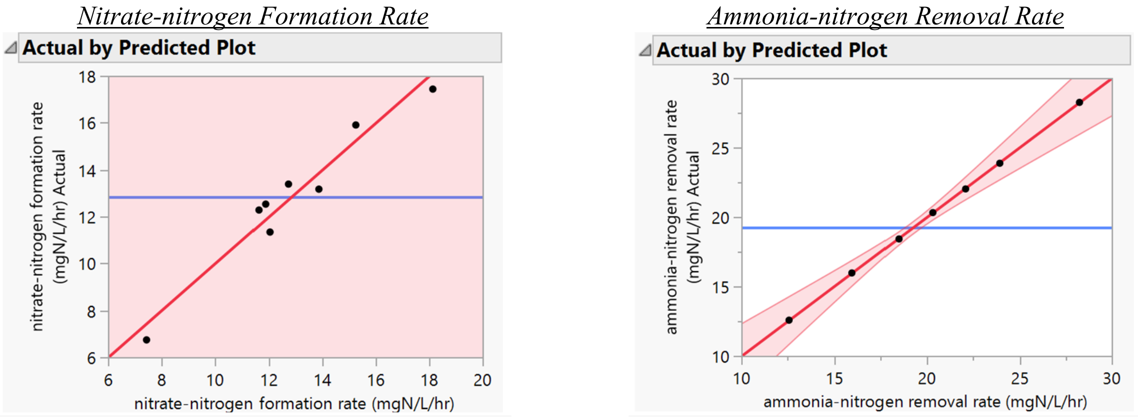

Nitrate-nitrogen Formation Rate — Summary of Fit

RSquare	0.948237
RSquare Adj	0.637656
Root Mean Square Error	1.914138
Mean of Response	12.861
Observations (or Sum Wgts)	8

Analysis of Variance

Source	DF	Sum of Squares	Mean Square	F Ratio
Model	6	67.118186	11.1864	3.0531
Error	1	3.663924	3.6639	Prob > F
C. Total	7	70.782110		0.4121

Effect Tests

Source	Nparm	DF	Sum of Squares	F Ratio	Prob > F
N_0 (mg/L)	1	1	11.887688	3.2445	0.3226
Initial COD/N	1	1	2.150738	0.5870	0.5838
pH	1	1	15.495745	4.2293	0.2881
N_0 (mg/L)*Initial COD/N	1	1	5.438402	1.4843	0.4375
N_0 (mg/L)*pH	1	1	2.892013	0.7893	0.5376
Initial COD/N*pH	1	1	29.253601	7.9842	0.2165

Ammonia-nitrogen Removal Rate — Summary of Fit

RSquare	0.999956
RSquare Adj	0.999693
Root Mean Square Error	0.09652
Mean of Response	19.26663
Observations (or Sum Wgts)	8

Analysis of Variance

Source	DF	Sum of Squares	Mean Square	F Ratio
Model	6	212.26102	35.3768	3797.377
Error	1	0.00932	0.0093	Prob > F
C. Total	7	212.27034		0.0124*

Effect Tests

Source	Nparm	DF	Sum of Squares	F Ratio	Prob > F
N_0 (mg/L)	1	1	18.828316	2021.046	0.0142*
Initial COD/N	1	1	86.257545	9258.951	0.0066*
pH	1	1	72.342406	7765.289	0.0072*
N_0 (mg/L)*Initial COD/N	1	1	31.924045	3426.751	0.0109*
N_0 (mg/L)*pH	1	1	1.626306	174.5689	0.0481*
Initial COD/N*pH	1	1	1.282401	137.6539	0.0541

Fig. 7. Least squares fit results for nitrate-nitrogen formation rate and ammonia-nitrogen removal rate.

The interaction profiles in Fig. 8 reveal that higher N_0 significantly enhances both ammonia removal and nitrate formation rates, with a more pronounced effect on ammonia oxidation. While an alkaline pH appears to slightly enhance nitrate formation under certain conditions, it does not consistently inhibit ammonia removal, suggesting that pH influences nitrogen transformation processes but not in a strictly opposing manner. The COD/N ratio strongly affects ammonia removal, where a lower COD/N of 0.5 supports higher removal rates, possibly due to reduced competition for oxygen and substrate availability. Additionally, non-parallel trends in nitrate formation profiles indicate significant interaction effects, particularly between pH and COD/N, suggesting microbial activity shifts under varying conditions. These findings were interpreted using principles of interaction effects, where non-parallel lines indicate significant factor interactions influencing response variables, as explained in [48, 49].

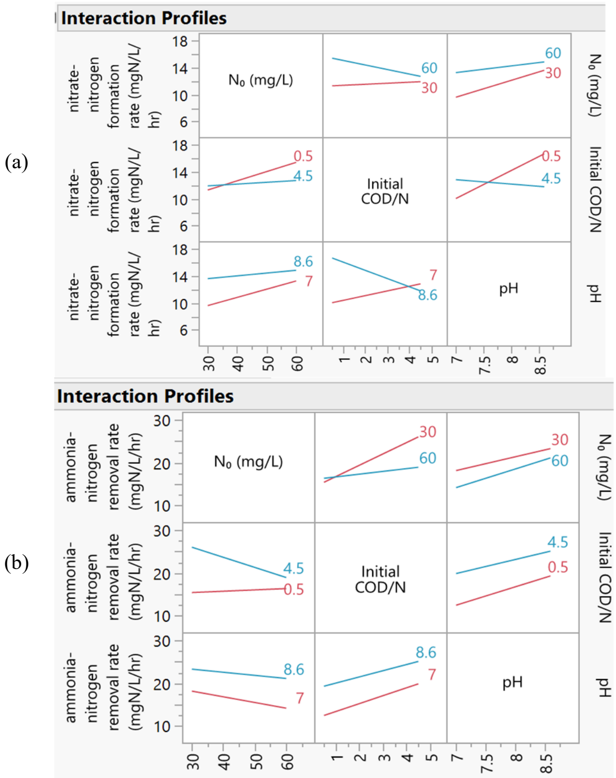

Fig. 8. Parameter interaction profile for (a) nitrate-nitrogen formation rate and (b) ammonia-nitrogen removal rate.

V. Conclusion

The results of this study demonstrate that CMX *Nitrospira* played a significant role in ammonia-nitrogen removal, particularly under high initial ammonia concentrations and specific COD/N and pH conditions. Leg 6 exhibited the highest CMX/AOB DNA ratio and the highest ammonia removal rate, as confirmed by both experimental results and JMP prediction profiling, which identified it as the optimal condition with a high desirability score of 99.77%. In contrast, lower initial ammonia concentrations correlated with lower CMX/AOB ratios, with Leg 1 showing the lowest ratio and the slowest ammonia removal rate. Minimal nitrite accumulation was observed across all experimental legs, with transient peaks in Leg 2 and Leg 6 reinforcing the hypothesis that CMX facilitated a direct ammonia-to-nitrate conversion, bypassing nitrite as an intermediate. Statistical analyses further confirmed that ammonia removal was significantly influenced by N_0, COD/N ratio, and pH (p = 0.0124, F-ratio = 3797.377), while nitrate formation rates showed no significant variation (p = 0.4121). These findings provide strong evidence that CMX-driven nitrification can be enhanced under specific conditions, contributing to improved efficiency in biological nitrogen removal.

Conflict of Interest

The authors declare no conflict of interest.

Author Contributions

TRL Panaligan designed the research framework, conducted data collection, and analyzed the results. YJ Wu provided mentorship, refining the framework and ensuring experimental accuracy. Prof. LM Whang facilitated collaboration and provided key resources, while BT Doma offered critical guidance. All authors contributed to data interpretation, manuscript review, and revisions.

Acknowledgment

The authors sincerely thank all Environmental Biotechnology Laboratory colleagues for their invaluable support, guidance, collaboration, and expertise, which were instrumental in the successful completion of the laboratory work at National Cheng Kung University.

References

[1] G. Salbitani and S. Carfagna, "Ammonium utilization in microalgae: A sustainable method for wastewater treatment," *Sustainability*, vol. 13, no. 2, p. 956, Jan. 2021. doi: 10.3390/su13020956

[2] J. Leszczyński, "Removal of ammonium ions from aqueous solutions using weathered halloysite," *Materials*, vol. 14, no. 16, pp. 4359, Aug. 2021. doi: 10.3390/ma14164359

[3] W. Lin *et al.*, "A review of the emerging risks of acute ammonia nitrogen toxicity to aquatic decapod crustaceans," *Water (Basel)*, vol. 15, no. 1, pp. 27, Dec. 2022. doi: 10.3390/w15010027

[4] Y. Huang *et al.*, "New insights into the mechanism of ammonia toxicity: Focus on Cactus," *Ecotoxicol Environ Saf*, vol. 249, 114357, Jan. 2023. doi: 10.1016/j.ecoenv.2022.114357

[5] M. Constable, M. Charlton, F. Jensen, K. McDonald, G. Craig, and K. W. Taylor, "An ecological risk assessment of ammonia in the aquatic environment," *Human and Ecological Risk Assessment: An International Journal*, vol. 9, no. 2, pp. 527–548, Mar. 2003. doi: 10.1080/713609921

[6] M. Á. Pérez-Martín, "Understanding nutrient loads from catchment and eutrophication in a salt lagoon: The Mar Menor case," *Water (Basel)*, vol. 15, no. 20, p. 3569, Oct. 2023. doi: 10.3390/w15203569.

[7] E. O. Igbinosa and A. I. Okoh, "Impact of discharge wastewater effluents on the physico-chemical qualities of a receiving watershed in a typical rural community," *International Journal of Environmental Science & Technology*, vol. 6, no. 2, pp. 175–182, Mar. 2009. doi: 10.1007/BF03327619.

[8] A. K. Maharjan, T. Kamei, I. M. Amatya, K. Mori, F. Kazama, and T. Toyama, "Ammonium-nitrogen (NH4+-N) removal from groundwater by a dropping nitrification reactor: Characterization of NH4+-N transformation and bacterial community in the reactor," *Water (Basel)*, vol. 12, no. 2, pp. 599, Feb. 2020. doi: 10.3390/w12020599.

[9] A. M. Richard, J. H. Diaz, and A. D. Kaye, "Reexamining the risks of drinking-water nitrates on public health," *Ochsner J*, vol. 14, pp. 392–398, 2014.

[10] Environment and climate change Canada, *Canadian Environmental Sustainability Indicators: Municipal Wastewater Treatment*, Aug. 2023.

[11] M. M. Mathew *et al.*, "Biological approaches integrating algae and bacteria for the degradation of wastewater contaminants—A review," *Front Microbiol*, vol. 12, Feb. 2022. doi: 10.3389/fmicb.2021.801051.

[12] N. P. M. Fontalvo, W. B. M. Gamero, H. A. M. Ardila, A. F. P. Gonzalez, C. G. Ramos, and A. E. P. Muñoz, "Removal of nitrogenous compounds from municipal wastewater using a bacterial consortium: an opportunity for more sustainable water treatments," *Water Air Soil Pollut*, vol. 233, no. 8, p. 339, Aug. 2022. doi: 10.1007/s11270-022-05754-y.

[13] H. Daims, S. Lücker, and M. Wagner, "A new perspective on microbes formerly known as nitrite-oxidizing bacteria," *Trends Microbiol*, vol. 24, no. 9, pp. 699–712, Sep. 2016. doi: 10.1016/j.tim.2016.05.004.

[14] S. Al-Ajeel, E. Spasov, L. A. Sauder, M. M. McKnight, and J. D. Neufeld, "Ammonia-oxidizing archaea and complete ammonia-oxidizing Nitrospira in water treatment systems," *Water Res X*, vol. 15, 100131, May 2022. doi: 10.1016/j.wroa.2022.100131.

[15] E. Spasov *et al.*, "High functional diversity among Nitrospira populations that dominate rotating biological contactor microbial communities in a municipal wastewater treatment plant," *ISME J*, vol. 14, no. 7, pp. 1857–1872, Jul. 2020. doi: 10.1038/s41396-020-0650-2.

[16] J. I. Prosser, "Autotrophic nitrification in bacteria," *Adv Microb Physiol.*, pp. 125–181, 1990. doi: 10.1016/S0065-2911(08)60112-5.

[17] G. A. Kowalchuk and J. R. Stephen, "Ammonia-oxidizing bacteria: A model for molecular microbial ecology," *Annu Rev Microbiol*, vol. 55, no. 1, pp. 485–529, Oct. 2001. doi: 10.1146/annurev.micro.55.1.485.

[18] B. B. Ward, "Nitrification in marine systems," in *Proc. Nitrogen in the Marine Environment*, Elsevier, 2008, pp. 199–261. doi: 10.1016/B978-0-12-372522-6.00005-0.

[19] M. Zheng *et al*., "Active ammonia-oxidizing bacteria and archaea in wastewater treatment systems," *Journal of Environmental Sciences*, vol. 102, pp. 273–282, Apr. 2021. doi: 10.1016/j.jes.2020.09.039.

[20] A. Palomo, A. Dechesne, O. X. Cordero, and B. F. Smets, "Evolutionary ecology of natural comammox Nitrospira populations," *mSystems*, vol. 7, no. 1, Feb. 2022. doi: 10.1128/msystems.01139-21.

[21] H. Daims *et al*., "Complete nitrification by Nitrospira bacteria," *Nature*, vol. 528, no. 7583, pp. 504–509, Dec. 2015. doi: 10.1038/nature16461.

[22] A. Prinčič, I. Mahne, F. Megušar, E. A. Paul, and J. M. Tiedje, "Effects of pH and oxygen and ammonium concentrations on the community structure of nitrifying bacteria from wastewater," *Appl Environ Microbiol*, vol. 64, no. 10, pp. 3584–3590, Oct. 1998. doi: 10.1128/AEM.64.10.3584-3590.1998.

[23] J. I. Prosser and G. W. Nicol, "Archaeal and bacterial ammonia-oxidisers in soil: the quest for niche specialisation and differentiation," *Trends Microbiol*, vol. 20, no. 11, pp. 523–531, Nov. 2012. doi: 10.1016/j.tim.2012.08.001.

[24] T. T. H. Le, J. Fettig, and G. Meon, "Kinetics and simulation of nitrification at various pH values of a polluted river in the tropics," *Ecohydrology & Hydrobiology*, vol. 19, no. 1, pp. 54–65, Jan. 2019. doi: 10.1016/j.ecohyd.2018.06.006.

[25] H.-D. Park and D. R. Noguera, "Evaluating the effect of dissolved oxygen on ammonia-oxidizing bacterial communities in activated sludge," *Water Res*, vol. 38, no. 14–15, pp. 3275–3286, Aug. 2004. doi: 10.1016/j.watres.2004.04.047.

[26] M.-Y. Jung *et al*., "Ammonia-oxidizing archaea possess a wide range of cellular ammonia affinities," *ISME J*, vol. 16, no. 1, pp. 272–283, Jan. 2022. doi: 10.1038/s41396-021-01064-z.

[27] M. Zielinska, K. Bernat, A. Cydzik-Kwiatkowska, J. Sobolewska, and I. Wojnowska-Baryla, "Nitrogen removal from wastewater and bacterial diversity in activated sludge at different COD/N ratios and dissolved oxygen concentrations," *Journal of Environmental Sciences*, vol. 24, no. 6, pp. 990–998, Jun. 2012. doi: 10.1016/S1001-0742(11)60867-X.

[28] L. A. Román-Ramírez and J. Marco, "Design of experiments applied to lithium-ion batteries: A literature review," *Appl Energy*, vol. 320, 119305, Aug. 2022. doi: 10.1016/j.apenergy.2022.119305.

[29] F. Yates, "Sir Ronald Fisher and the design of experiments," *Biometrics*, vol. 20, no. 2, p. 307, Jun. 1964. doi: 10.2307/2528399.

[30] B. Durakovic, "Design of experiments application, concepts, examples: State of the art," *Periodicals of Engineering and Natural Sciences (PEN)*, vol. 5, no. 3, Dec. 2017. doi: 10.21533/pen.v5i3.145.

[31] C. Kamath, "Data mining and statistical inference in selective laser melting," *The International Journal of Advanced Manufacturing Technology*, vol. 86, no. 5–8, pp. 1659–1677, Sep. 2016. doi: 10.1007/s00170-015-8289-2.

[32] Y. Hao, V. C. Tai, and Y. C. Tan, "A systematic stereo camera calibration strategy: Leveraging Latin hypercube sampling and 2k full-factorial design of experiment methods," *Sensors*, vol. 23, no. 19, pp. 8240, Oct. 2023. doi: 10.3390/s23198240.

[33] J. Antony, "Full factorial designs," in *Proc. of Design of Experiments for Engineers and Scientists*, Elsevier, 2023, pp. 65–87. doi: 10.1016/B978-0-443-15173-6.00009-3.

[34] F. D. O. Riswanto, A. Rohman, S. Pramono, and S. Martono, "Application of response surface methodology as mathematical and statistical tools in natural product research," *J Appl Pharm Sci*, vol. 9, no. 10, pp. 125–133, Oct. 2019. doi: 10.7324/JAPS.2019.91018.

[35] J. H. Rotthauwe, K. P. Witzel, and W. Liesack, "The ammonia monooxygenase structural gene amoA as a functional marker: molecular fine-scale analysis of natural ammonia-oxidizing populations," *Appl Environ Microbiol*, vol. 63, no. 12, pp. 4704–4712, Dec. 1997. doi: 10.1128/aem.63.12.4704-4712.1997.

[36] M. Wang, G. Huang, Z. Zhao, C. Dang, W. Liu, and M. Zheng, "Newly designed primer pair revealed dominant and diverse comammox amoA gene in full-scale wastewater treatment plants," *Bioresour Technol*, vol. 270, pp. 580–587, Dec. 2018. doi: 10.1016/j.biortech.2018.09.089.

[37] W. S. Sjah, B. Rahman, D. Hindarto, and A. B. P. B. Wedha, "Diagnostic on car internal combustion engine through noise," *SinkrOn*, vol. 8, no. 2, pp. 1128–1139, May 2023. doi: 10.33395/sinkron.v8i2.12392.

[38] M. W. Liemohn, A. D. Shane, A. R. Azari, A. K. Petersen, B. M. Swiger, and A. Mukhopadhyay, "RMSE is not enough: Guidelines to robust data-model comparisons for magnetospheric physics," *J Atmos Sol Terr Phys*, vol. 218, 105624, Jul. 2021. doi: 10.1016/j.jastp.2021.105624.

[39] G. Romeo, "Data analysis for business and economics," *Elements of Numerical Mathematical Economics with Excel*, Elsevier, 2020, pp. 695–761. doi: 10.1016/B978-0-12-817648-1.00013-X.

[40] A. Özkan, K. Özkan, Ş. Işık, and M. Banar, "Evaluation of different curve fitting models for prediction of municipal solid waste composition," *Pamukkale University Journal of Engineering Sciences*, vol. 27, no. 3, pp. 385–393, 2021. doi: 10.5505/pajes.2020.08377.

[41] M. A. H. J. van Kessel *et al.*, "Complete nitrification by a single microorganism," *Nature*, vol. 528, no. 7583, pp. 555–559, Dec. 2015. doi: 10.1038/nature16459.

[42] O. Zajac, M. Zubrowska-Sudol, M. Godzieba, and S. Ciesielski, "Changes in Nitrification Kinetics and Diversity of Canonical Nitrifiers and Comammox Bacteria in a Moving Bed Sequencing Batch Biofilm Reactor—A Long-Term Study," *Water (Basel)*, vol. 16, no. 4, p. 534, Feb. 2024. doi: 10.3390/w16040534.

[43] T. R. L. Panaligan, A. K. S. Lee, C. J. Petareal, and J. R. Tadena, "Synthesis, Characterization, and Utilization of Water Hyacinth (Eichhornia crassipes) Magnetic Biochar for Nitrate Removal from Simulated Wastewater," *Key Eng Mater*, vol. 980, pp. 81–86, Apr. 2024. doi: 10.4028/p-MQqs5n.

[44] K. D. Kits *et al*., "Kinetic analysis of a complete nitrifier reveals an oligotrophic lifestyle," *Nature*, vol. 549, no. 7671, pp. 269–272, Sep. 2017. doi: 10.1038/nature23679.

[45] H. Koch, M. A. H. J. van Kessel, and S. Lücker, "Complete nitrification: insights into the ecophysiology of comammox Nitrospira," *Appl Microbiol Biotechnol*, vol. 103, no. 1, pp. 177–189, Jan. 2019. doi: 10.1007/s00253-018-9486-3.

[46] D. Li, W. Liang, X. Sun, W. Sun, G. Liu, and E. Y. Zeng, "Long-term stability of comammox Nitrospira under weakly acidic conditions and their acid-adaptive mechanisms revealed by genome-centric metatranscriptomics," *Bioresour Technol*, vol. 418, Feb. 2025. doi: 10.1016/j.biortech.2024.131986.

[47] S. Xu, W. Chai, R. Xiao, B. F. Smets, A. Palomo, and H. Lu, "Survival strategy of comammox bacteria in a wastewater nutrient removal system with sludge fermentation liquid as additional carbon source," *Science of The Total Environment*, vol. 802, 149862, Jan. 2022. doi: 10.1016/j.scitotenv.2021.149862.

[48] JMP 18.1 Help. (Mar. 29, 2025). [Online]. Available: https://www.jmp.com/support/help/en/18.1/index.shtml#page/jmp/interaction-plots.shtml

[49] Interpret the key results for Interaction Plot – Minitab. (Mar. 29, 2025). [Online]. Available: https://support.minitab.com/en-us/minitab/help-and-how-to/statistical-modeling/anova/how-to/interaction-plot/interpret-the-results/key-results/

Copyright © 2025 by the authors. This is an open access article distributed under the Creative Commons Attribution License which permits unrestricted use, distribution, and reproduction in any medium, provided the original work is properly cited (CC BY 4.0).